




Spontaneous Resolution and Super-coiling in Xerogels of the Products of Photo-Induced Formose Reaction

Sergey V. Stovbun¹ · Anatoly M. Zanin¹ · Mikhail V. Shashkov^{2,3} · Aleksey A. Skoblin¹ · Dmitry V. Zlenko^{1,4}  · Vsevolod A. Tverdislov⁵ · Marya G. Mikhaleva¹ · Oxana P. Taran^{2,3} · Valentin N. Parmon^{2,3,6}

Received: 20 February 2019 / Accepted: 17 July 2019 /

Published online: 22 October 2019

© Springer Nature B.V. 2019

Abstract

This work addresses the supramolecular self-organization in the xerogels of formose reaction products. The UV-induced formose reaction was held in over-saturated formaldehyde solutions at 70 °C without a catalyst. The solutions of the obtained carbohydrates were dried on a glass slide, and the obtained xerogels demonstrated a prominent optical activity, while the initial solutions were optically inactive. The xerogels contained highly elongated crystalline elements of a helical structure as well as the isometric ones. Thus xerogel formation was accompanied by a spontaneous resolution of enantiomers and separation of different-shaped supramolecular structures. The thick helices were twisted of thinner ones, while the latter were twisted of elementary structures having a diameter much smaller than 400 nm. Similar structural hierarchy is typical of biological macromolecules (DNA, proteins, and cellulose). Summarizing the obtained results, we proposed a hypothetical mechanism explaining the amplification of the initial enantiomeric excess, as well as chiral and chemical purification of the substances which were essential for the evolution of Life to start.

Keywords Self-assembly · Formose reaction · Supercoiling

Modeling the early stages of life development faces two main challenges, since the reactions leading to biological molecules produce complex mixtures of a wide range of organic

✉ Dmitry V. Zlenko
dvzlenko@gmail.com

¹ N.N. Semenov Institute of Chemical Physics, RAS, 119991, Kosygina 4, Moscow, Russia

² G.K. Boreskov Institute of Catalysis SB RAS, 630090, Lavrentiev Avenue 5, Novosibirsk, Russia

³ Novosibirsk State University, 630090, Pirogova 1, Novosibirsk, Russia

⁴ Faculty of Biology, M.V. Lomonosov Moscow State University, 119192, Lenin Hills 1/12, Moscow, Russia

⁵ Faculty of Physics, M.V. Lomonosov Moscow State University, 119234, Lenin Hills 1/2, Moscow, Russia

⁶ Tomsk State University, 634050, Lenin Avenue 36, Tomsk, Russia

compounds (Kitadai and Maruyama 2018). First comes the problem of how individual chemical substances got separated that is the prerequisite for evolution to start (Schwartz 2007). The second is how enantiomers diverged since chirality is the fundamental property of modern life (Schwartz 2007; Kuhn 2008). The separation of both enantiomers and chemical substances could result from amplification of the initial asymmetry, when some amount of the oligomers capable of replication is already present in the system. In this case, the replication of the homochiral oligomers outperforms the replication of their racemic analogs, which leads to an increased concentration of the former, and, in the long run, to the natural selection of the most “adapted” chiral oligomers (Joyce et al. 1984; Bolli et al. 1997; Kuhn 2008; Avalos et al. 2010). However, the origin of the initial chiral replicable oligomers stays unclear. Moreover, the “replication” mechanism of the chirality amplification is complicated by the “enantiomeric cross-inhibition”, a phenomenon of the strong retardation of the chiral oligomers replication by a small amount of the enantiomers of the opposite sign (Joyce et al. 1984). So, the “replication” mechanism of the chirality amplification seems to require the preexisting chirally-pure solution.

The chemistry of the processes that could have been proceeding on the young Earth and leading to the biological compounds is well known and was described in numerous works (Orgel 2004; Schwartz 2007; Kitadai and Maruyama 2018). One of the ways to drive the carbohydrate abiotic synthesis is the formose reaction (Orgel 2004; Schwartz 2007; Kim et al. 2011; Ritson and Sutherland 2012; Kitadai and Maruyama 2018): a formaldehyde condensation in the presence of Ca^{2+} or OH^- ions (Butlerow 1861). It includes three main stages involving the carbonyl group: 1. deprotonation of the α -carbon atom (enolization); 2. the nucleophilic attack of the resulting enolate on the carbonyl group leading to a new C-C bond (aldol condensation); 3. retro-aldol fragmentation resulting in the cleavage of the molecules (Kim et al. 2011; Ritson and Sutherland 2012; Kitadai and Maruyama 2018). The first stage requires alkaline conditions ($\text{pH} > 10$) and proceeds in the presence of metal ions (Kitadai and Maruyama 2018). The formose reaction brings about a wide range of carbohydrates and under certain conditions – even to ribose and some hexoses common for a living cells (Breslow 1959; Decker et al. 1982; Kim et al. 2011). The formose reaction can be initiated by the UV exposure in the presence of a metal catalyst (Shigemasa et al. 1977; Ritson and Sutherland 2012) or without it (Snytnikova et al. 2006). In both cases, a broad range of different carbohydrates was observed among the products.

In the presence of chiral catalysts (such as aminoacids), the formose reaction itself may lead to the stereochemically asymmetric products (Northrup et al. 2004). The origin of such catalysts is still under discussion (it could be even extraterrestrial Pizzarello and Weber 2004; Breslow and Cheng 2009; Glavin and Dworkin 2009), as the emergence of the initial chirality and/or initial Enantiomeric Excess (EE) stays a key problem (Burton et al. 2012). The symmetry could break in formose reaction due to the peculiarities of the kinetics of the aldol-condensation stage (Frank 1953; Mauksch et al. 2007, 2009). This mechanism can lead to EE of 10–15 % in a single iteration (Mauksch et al. 2009) that is a very significant asymmetry allowing to be amplified further in a chain of repetitive iterations.

The mechanism of symmetry breaking proposed by Prigogine for the systems being far from the equilibrium (Nicolis and Prigogine 1981) is similar to the mechanism proposed by Frank (1953) and observed by Mauksch et al. (2007, 2009). This scheme is realized in the auto-catalytic chiral crystallization of the sodium chlorate under stirring. The phenomenon was explained by the “secondary” nucleation, when the existing “mother” crystal imposes the way of crystallization for other small crystals (Kipping and Pope 1898; Kondepudi et al. 1990). This effect coupled with the conglomerates’ resolution described by Viedma (2005, 2007) allowed to suppose that the key initial steps of chemical evolution

were heterogeneous (Avalos et al. 2010). This supposition chimes with the putative role of the molecular self-organization at the early stages of the chemical evolution (Eigen 1971).

In this work, we characterize the products of the photo-induced formose reaction held in a concentrated aqueous formaldehyde solution. We did not use any catalysts or add other additional components to avoid the possible influence of the initial mixture chirality on the chirality of the final products. Particular attention was paid to the structure of the optically active crystalline phase formed by the formose reaction products after the solvent evaporated. We observed the spontaneous resolution and conglomerate formation in the course of crystallization (Schwartz 2007; Srisanga and ter Horst 2010), followed by supramolecular self-organization and probably purification of the individual chemical substances. So, we observed a simultaneous realization of all three key stages of the chemical evolution: synthesis, resolution, and purification during a single process. We believe that our observations are of crucial importance to unlock the “mechanics” of the origin of Life on Earth.

Materials and Methods

The 95 % formaldehyde aqueous solution was prepared by heating paraformaldehyde at 160–170 °C (1.5 hour). The formose reaction was held at 70 °C for 8.5 hours under permanent UV illumination. The DRSH-100 mercury lamp was used for the UV irradiation of the samples. The lamp was placed 10 cm above the surface of the formaldehyde solution. The reaction was considered as completed after the full setting of the solution and was repeated 5 times independently.

The main product of the reaction was paraformaldehyde that was removed by vacuum sublimation (80 °C, 250 hours). The mass of the nonvolatile residue after paraformaldehyde sublimation was at least 0.7 % of the initial dry weight. The obtained substance was partially soluble in water at the room temperature. The water-soluble fraction (“Product” here and hereafter) was separated from water-insoluble fraction by dissolution in distilled water followed by evaporation. The water-insoluble fraction was not analyzed, as carbohydrates and polyatomic alcohols are the water-soluble substances. Most probably, the water-insoluble residue was composed mainly of the residual paraformaldehyde. The fresh Fehling’s solution (von Fehling 1848) analysis was used for the qualitative identification of the reducing carbohydrates in the Product. The phase transition temperatures were determined using mercury thermometer (100–200 °C, sensitivity 1 °C).

Dried Product was derivatized with Bis(trimethylsilyl)amine and (chloromethyl)silane (Sweeley et al. 1963) using sorbitol as an internal standard. The chemical composition of the derivatized Product was analyzed using Agilent GC 7890 gas chromatograph (HP-5MS capillary column: 30 m x 0.25 mm, and 0.25 μ m film thickness) coupled with Agilent 7000B triple quadrupole mass spectrometer (Agilent Technologies, USA). Oven temperature linearly grew from 80 °C up to 280 °C within the experiment (8 °C/min). The Golm Metabolome Database (Hummel et al. 2007) was used to identify substances. Helium (99.9999 %) was used as the carrier gas.

The xerogels of the Product were obtained by slow (12 hours, typically) drying of a thin layer of the diluted samples on a glass slide. The process was held at a room temperature in a dust-free air atmosphere. This technique allowed obtaining the crystalline structures on the glass surface, while no solid phase particles were observed in the initial liquid Product (see the Results section). Similar effects of the supramolecular self-assembly were observed earlier in solutions of the N-trifluoroacetylated α -amioalcohols (Stovbun et al. 2012).

The optical-microscopy analysis of the Product's xerogels was made using MIKMED-6 optical microscope equipped with a crossed polarizers. To prove the conglomerate formation, we examined the xerogels through the analyzer-polarizer pair turned 3° left or right with respect to their full crossed orientation ("semi-crossed" polarizers). This allowed observing structures having opposite signs of the polarization plane rotation. The value of 3° was used as it allowed to obtain the most contrast images.

Results

Compounds Description

After paraformaldehyde sublimation, we obtained a beige-brownish substance insoluble in ethyl acetate, acetone, glycerol, as well as in the ammonia and hydrogen peroxide solutions. Still, this substance was poorly soluble in water and freely soluble in benzene, cyclohexane, chloroform, and carbon tetrachloride. At the room temperature, the water-soluble fraction of the formose reaction product (Product) was a viscous liquid of white color having a boiling temperature of $118 \pm 5^\circ\text{C}$ (1 Bar). The water-insoluble fraction of the reaction product was a crystalline compound of beige color having a melting temperature of $138 \pm 5^\circ\text{C}$ that lay in the range reported for the melting point of paraformaldehyde ($120\text{--}170^\circ\text{C}$, Sigma-Aldrich, P6148). The aqueous solutions of the Product were optically inactive that indicated them to be the racemic mixtures.

Composition of the Product

The fresh Fehling's solution (von Fehling 1848) treatment revealed the reducing carbohydrates in the Product. The GC/MS chromatography of the Product revealed a complex mixture of different substances. Only several substances were identified as carbohydrates and polyalcohols: glycolic acid and aldehyde, glycerol, and fructose (Fig. 1a). The chemical structure of the substances was confirmed by mass-spectrometry (Fig. 1b and c). Thus, in our experiments, a significant part of the substances among the formose reaction products appeared to be carbohydrates and the related compounds.

Optical Activity of the Xerogel

The xerogels of the Product were prepared by drying of the diluted samples on the glass slide (Fig. 2). Observing the xerogels through the crossed analyzer-polarizer pair revealed the optically active structures seen as bright images at the dark background. A comprehensive study of numerous (about 100) samples revealed only a few structures that did not demonstrate any detectable optical activity. The microscopic observation of the xerogels also revealed a range of the structures having different optical properties and shapes. We observed both highly elongated fiber-like (anisometric) elements (Fig. 2a,b,e-h) and flat structures (Fig. 2c,d). Scratching the obtained xerogels with a needle showed that the observed structures were fragile. So, we assumed them to be of a crystalline or quasi-crystalline structure. With that, the absence of the rainbow coloring in the images (Fig. 2) denotes that the characteristic size of the elementary crystalline regions was much smaller than the wavelength of the visible light (400 nm, Kleman and Laverntovich 2004).

When the polarizer and analyzer were "semi-crossed" (turned 3° left or right in respect of their fully-crossed orientation), some of the structures were bright when the analyzer

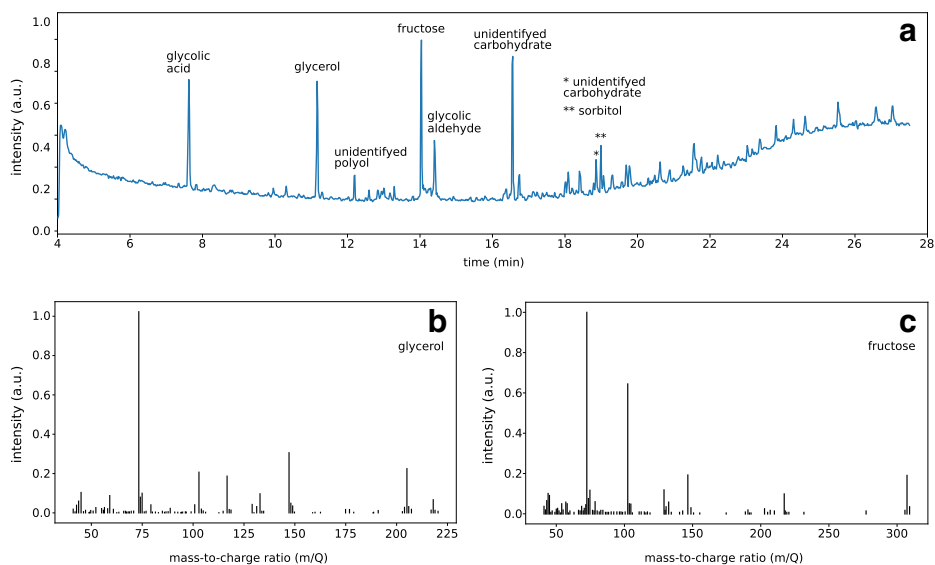


Fig. 1 **a** Typical chromatogram of the Product. Most of the obtained minor substances were not identified and were not labeled. **b** and **c** Full-scale mass spectra of the siliconated derivatives of the typical substances revealed and definitely identified in the Product mixture

was turned right and dark when the analyzer was turned left (laevorotatory, Fig. 2b,c,e,f, red marks). We also observed structures having an opposite optical activity and visible as bright in case of a left-turned analyzer (dextrorotatory, Fig. 2a,d,e,f, green marks). There were also anisometric structures visible as bright in both cases (Fig. 2g,h, blue marks). The anisometric structures of the former type (changing their brightness with the analyzer turn) were always “thin” having a diameter of about several micrometers, while the structures of the latter one were always “thick” with a diameter of about 10 μm .

The visibility of the thick structures under both “semi-crossed” polarizer-analyzer pair orientations could be explained by the intense light scattering by the nonideal polarizers. To verify this possibility, we prepared the achiral crystalline xerogel (simple NaCl) under the same conditions as for the Product and examined it using the same microscope. In the achiral xerogel, we did not observe any bright objects with the given angles of the polarizer and analyzer (data not shown). Thus, light scattering cannot explain the observed phenomenon.

Microscopic investigation clearly demonstrated that xerogels contained crystalline structures with the opposite optical activity. Given that the solutions of the Product were optically inactive, the enantiomers underwent spontaneous splitting, and the resulting xerogels were conglomerates.

Helicity of the Crystal-Like Structures

Often, the elongated crystal-like structures had a prominent helical structure (Fig. 2e-h). Moreover, according to the microscopic observations, thick structures seem to be twisted from several thinner ones (Fig. 2g,h). The latter, in their turn, also seem to be twisted of numerous elementary structures having a diameter of several (or several dozens) of

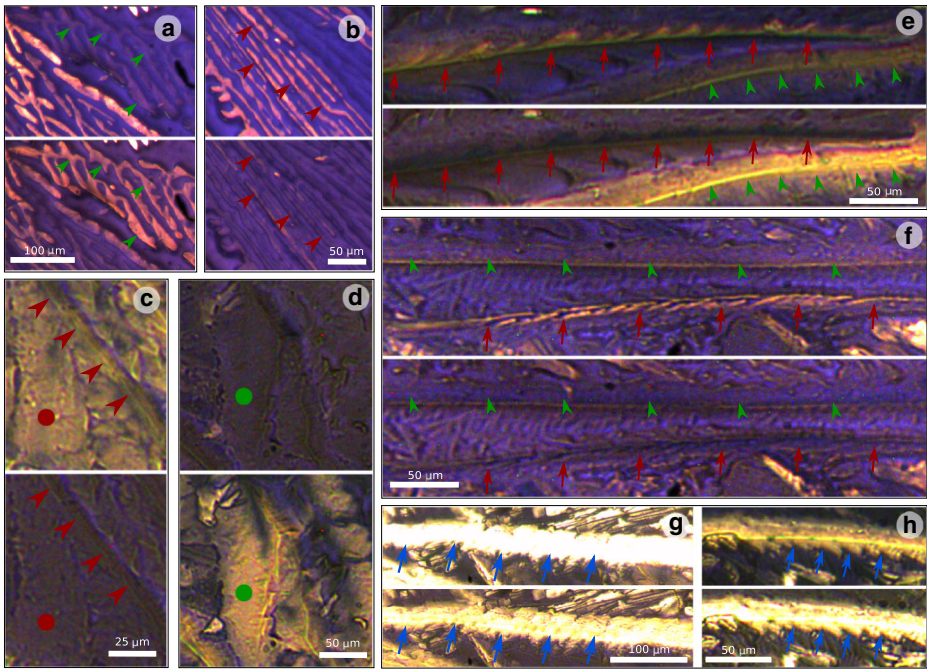


Fig. 2 Typical optical microscopy images of the Product xerogel, obtained through the “semi-crossed” analyzer-polarizer pair. There are two images of the same field of view in each panel: the top image was obtained with the analyzer turned 3° to the right, and the bottom image was obtained with the analyzer turned 3° to the left. Red marks denote thin laevorotatory structures, while the green marks denote thin dextrorotatory ones, blue marks denote thick structures. Dots mark the flat structures, arrowheads denotes the anisometric structures, and arrows mark the helical structures. **a** Anisometric dextrorotatory structures (green arrowheads); **b** Anisometric laevorotatory structures (red arrowheads); **c** Anisometric (red arrowheads) and flat (red dot) laevorotatory structures; **d** Flat dextrorotatory structure (green dot); **e** and **f** Thin helical laevorotatory (red arrows) and anisometric dextrorotatory (green arrowheads) structures; **g** Thick laevorotatory helical structure (blue arrows); **h** Thick dextrorotatory helical structure (blue arrows)

nanometers, since the characteristic size of the elementary crystalline elements was much smaller than the visible light wavelength ($\ll 400$ nm).

Going back to the problem of visibility of the thick structures under different analyzer orientations we can note, that their brightness was not equal. This fact implies that the thick structures are also optically active. So, the greater thickness and greater optical path through the thick structures can explain both their visibility under both analyzer orientations, and the difference in their brightness. Indeed, the greater optical path implies greater rotational angle and if this angle is large enough, the object would be visible in both cases.

According to our observations, the helical structures having the different swirl direction demonstrated the opposite optical activity. For example, in Fig. 2g (blue arrows), the thick fiber is a left-handed helix, while, in Fig. 2h, the thick fiber is a right-handed one. And they demonstrate the opposite optical activity: the fiber in Fig. 2g rotated the polarization plane to the left, while the fiber in Fig. 2h – to the right. The thin helical fibers also demonstrated clearly visible helical structure that was also related to the sign of their optical activity. For example, in Fig 2e and f, the thin structures marked by red arrows were laevorotatory left helices. So, the swirl direction correlated with the rotation direction of polarization plane.

The latter conclusion is related to the magnitude of optical activity of the crystal-like elements observed in our experiments. This magnitude was much higher than it should be, according to the usual specific optical activities of natural carbohydrates. Indeed, given that the thickness h of the structures was about $10\ \mu\text{m}$, the rotation angle ϕ is $\sim 3^\circ$ (as such angle between the polarizer and analyzer brought the brightest images), and the density $\rho \sim 1.5\ \text{g/cm}^3$, the specific rotation α would be:

$$\alpha = \frac{\phi}{h\rho} \sim 20\,000, \frac{\text{deg} \cdot \text{ml}}{\text{g} \cdot \text{dm}}$$

that is at least two orders of magnitude greater than characteristic specific rotations of glucose and fructose: ~ 53 and $92\ (\text{deg ml})/(\text{g dm})$, for example (Weast 1974). The observed discrepancy could be explained by increasing the optical activity (both polarization plane rotation and circular dichroism) due to the delocalization of the electrons caused by electrostatic interaction of the absorbing molecules densely packed in condensed phase (Pescitelli et al. 2014). So, the helical packing of the molecules seems to amplify the optical activity in the crystal-like structures and, probably, determines its sign.

Discussion

Hierarchy of Chiral Supramolecular Packing

The optically active helical structures found in the Product xerogels strongly resemble the one-dimensional supramolecular structures (strings) that are formed by the N-trifluoroacetylated α -aminoalcohols (TFAAAs) in the course of solutions' cooling or thin layer drying (Stovbun et al. 2018). The strings have a helical structure and demonstrate optical activity, the TFAAA molecules in the strings are not covalently bound and form the strings due to the chirality-driven self-assembly (Stovbun et al. 2018). Moreover, the optical activity of the strings is determined by the supramolecular packing of the TFAAA molecules, rather than by their own molecular optical activity. The carbohydrate products of the formose reaction (Fig. 1) were chiral and formed similar helical anisometric crystalline structures (Fig. 2). Thus, there is a clear analogy in the behavior of these two different chemical substances that seems to reflect some fundamental physical principle.

One of the possible candidates for the principle that drives the formation of the helical structures during the chiral substances precipitation and self-assembly is a restriction of the available combinations for the complementary packing of the chiral molecules (Tverdislov et al. 2017). In particular, this restriction leads to superhelices being formed, as described for the proteins and nucleic acids (Tverdislov et al. 2017), the cellulose (Nikolsky et al. 2019), and TFAAAs (Stovbun et al. 2018). In the xerogels of the Product, the thick anisometric structures were composed of the thinner ones, while the latter were twisted of the elementary structures. So, the elementary, thin, and thick anisometric structures corresponded to three hierarchical structural levels, and the thinnest structure's diameter coincided with the thinnest biological helices by the order of magnitude. Unfortunately, the pure ribose, as well as other biological carbohydrates, have not formed any structures in the xerogels prepared via the same method as for formose reaction Product (data not shown). To our knowledge, such anisometric structures were not reported for pure carbohydrates. This fact forces us to propose, that the supramolecular self-assembly becomes possible only in complex mixtures of carbohydrates due to the interaction among the molecules of different chemical species.

Self-Assembly and Natural Selection

Finally, we would like to propose a hypothetical mechanism that could provide for a complete segregation of the substances that is essential for further evolution of Life. In the Product xerogels, we have observed both isometric (Fig. 2c,d, dots) and anisometric (Fig. 2a,b,e-h, arrows) structures. The difference in shape between them would result in their different mobility under any kind of external mechanical action. In general, the elongated structures have a greater surface/mass ratio and should be more mobile under the flow influence, waves action, or whatever might have transferred them. Let's suppose that the environmental conditions on the young Earth were changing cyclically, and in some periods the initial solution became oversaturated. In this case, the substances in the initial complex mixture should periodically precipitate, and the mechanical sorting can be a reason for the spatial segregation of the isometric and anisometric particles. As a result, after sufficient number of iterations, the anisometric and isometric particles could be concentrated in drastically different locations. In this regard, the ability for self-assembly becomes the key feature, as this ability determines the rheological properties of the resulting precipitate and the ability to segregate from other molecules and accumulate in some restricted areas.

Recently, we have described a phenomenon of the amplification of the initially small enantiomeric excess (EE) in the heterochiral solutions of TFAAAs (Zlenko et al. 2019). We were investigating close-to-racemic solutions and observed the precipitation of the isometric racemic residual, while the rest of the solution became chiral. The initial solution with small EE, in this case, transformed to a less concentrated but more or less pure solution of one of the enantiomers (which was initially in an excess). Moreover, if the concentration of the resulting chiral solution exceeded some critical value, the chiral TFAAA also precipitated but in the form of anisometric helical strings. So, the precipitate was composed both of racemic isometric and chiral anisometric particles. The latter demonstrates a clear analogy with the behavior found in the mixture of the formose reaction Product. If we suppose, that some ancestor carbohydrates were able to form an isometric racemic and anisometric chiral precipitates, they could have been separated from all other components of the initial complex mixture and become chemically and chirally pure due to the mechanical sorting. This mechanism naturally explains both the chiral purity of the biological molecules and selection of some particular molecules from the wide range of the substances synthesized in prebiotic age.

Our hypothesis implies that the ability to form anisometric chiral structures was an inherent property of the prebiotic molecules that became the ancestors of the modern biological molecules. From this point of view, the ability for the self-assembly (which is of crucial importance for modern life) could be considered as a kind of preadaptation for further complication of structure and diversification of functions in a living cell. Consequently, our hypothesis implies that the formation of the elongated helical structures (such as α -helices or double helix of DNA) preceded the polymerization of the monomers and appearance of the macromolecules themselves. Moreover, the shape of helical supramolecular structures seems to promote the formation of linear polymer chains. This effect was recently used for the flat (2D) polymers synthesis: the polymerization was initiated by UV irradiation after self-assembly of the monomers into a 2D structure (Kissel et al. 2012). Thus, the structure can guide the way the molecules to polymerize.

Acknowledgments The work was supported by FASO Russia, theme number 45.9, 0082-2014-0011, AAAA-17-117111600093-8.

References

- Avalos M, Babiano R, Cintas P, Jimenez JL, Palacios JC (2010) Homochirality and chemical evolution: new vistas and reflections on recent models. *Tetrahedron* 21:1030–1040
- Bolli M, Micurari R, Eschenmoser A (1997) Pyranosyl-rna: chiroselective self-assembly of base sequences by ligative oligomerization of tetranucleotide-2',3'-cyclophosphates (with a commentary concerning the origin of biomolecular homochirality). *Chem Biol* 4(4):309–320
- Breslow R (1959) On the mechanism of formose reaction. *Tetrahedr Lett* 21:22–26
- Breslow R, Cheng ZL (2009) On the origin of terrestrial homochirality for nucleosides and amino acids. *Proc Natl Acad Sci USA* 106(23):9144–9146
- Burton AS, Stern JC, Elsila JE, Glavin DP, Dworkin JP (2012) Understanding prebiotic chemistry through the analysis of extraterrestrial amino acids and nucleobases in meteorites. *Chem Soc Rev* 41(16):5459–5472
- Butlerow A (1861) Bildung einer zuckerartigen substanz durch synthese. *Eur J Org Chem* 120(3):295–298
- Decker P, Schweer H, Pohlmann R (1982) Bioids: X. identification of formose sugars, presumable prebiotic metabolites, using capillary gas chromatography/gas chromatography—mass spectrometry of n-butoxime trifluoroacetates on ov-225. *J Chrom A* 224(2):281–291
- Eigen M (1971) Selforganization of matter and the evolution of biological macromolecules. *Naturwissenschaften* 58(10):465–523
- von Fehling HC (1848) Quantitative bestimmung des zuckers im harn. *Archiv für physiologische Heilkunde* 7:64–73
- Frank F (1953) On spontaneous asymmetric synthesis. *Biochim Biophys Acta* 11:459–463
- Glavin DP, Dworkin JP (2009) Enrichment of the amino acid L-isovaline by aqueous alteration on CI and CM meteorite parent bodies. *Proc Natl Acad Sci USA* 106(14):5487–5492
- Hummel J, Selbig J, Walther D, Kopka J (2007) The golm metabolome database: a database for gc-ms based metabolite profiling. In: Nielsen J, Jewett MC (eds) *Metabolomics. A powerful tool in systems biology*, vol 4. Springer, Berlin, pp 75–95
- Joyce G, Visser G, van Boeckel C, van Boom J, Orgel L, van Westrenen J (1984) Chiral selection in poly(C)-directed synthesis of poly(G). *Nature* 310:602–604
- Kim HJ, Ricardo A, Illangkoon HI, Kim MJ, Carrigan MA, Frye F, Benner SA (2011) Synthesis of carbohydrates in mineral-guided prebiotic cycles. *J Am Chem Soc* 133(24):9457–9468
- Kipping FS, Pope WJ (1898) Enantiomorphism. *J Chem Soc Trans* 73:606–617
- Kissel P, Erni R, Schweizer WB, Rossell MD, King BT, Bauer T, Götzinger S, Schlüter AD, Sakamoto J (2012) A two-dimensional polymer prepared by organic synthesis. *Nat Chem* 4(4):287–291
- Kitadaï N, Maruyama S (2018) Origins of building blocks of life: a review. *Geosci Front* 9:1117–1153
- Kleman M, Laverntovich O (2004) *Soft matter physics. An introduction*. Springer, New York
- Kondepudi DK, Kaufman RJ, Sing N (1990) Chiral symmetry breaking in sodium chlorate crystallization. *Science* 250(4983):975–976
- Kuhn H (2008) Origin of life — symmetry breaking in the universe: emergence of homochirality. *Curr Opin Coll Int Sci* 13(1–2):3–11
- Mauksch M, Tsogoeva SB, Wei S, Martynova IM (2007) Demonstration of spontaneous chiral symmetry breaking in asymmetric mannich and aldol reactions. *Chirality* 19:816–825
- Mauksch M, Wei S, Freund M, Zamfir A, Tsogoeva SB (2009) Spontaneous mirror symmetry breaking in the aldol reaction and its potential relevance in prebiotic chemistry. *Orig Life Evol Biosph* 40:79–91
- Nicolis G, Prigogine I (1981) Symmetry breaking and pattern selection systems in far-from-equilibrium. *Proc Natl Acad Sci USA* 78(2):659–663
- Nikolsky SN, Zlenko DV, Melnikov VP, Stovbun SV (2019) The fibrils untwisting limits the rate of cellulose nitration process. *Carbohydr Polym* 204:232–237
- Northrup AB, Mangion IK, Hetteche F, MacMillan DW (2004) Enantioselective organocatalytic direct aldol reactions of α -oxaldehydes: step one in a two-step synthesis of carbohydrates. *Angew Chem Int Ed* 43:2152–2154
- Orgel LE (2004) Prebiotic chemistry and the origin of the rna world. *Crit Rev Biochem Mol Biol* 39:99–123
- Pescitelli G, Bari LD, Berova N (2014) Application of electronic circular dichroism in the study of supramolecular systems. *Chem Soc Rev* 43(15):5311–5233
- Pizzarello S, Weber AL (2004) Prebiotic amino acids as asymmetric catalysts. *Science* 303(5661):1151
- Ritson D, Sutherland JD (2012) Prebiotic synthesis of simple sugars by photoredox systems chemistry. *Nature* 4(11):895–899
- Schwartz AW (2007) Intractable mixtures and the origin of life. *Chem Biodivers* 4:656–664
- Shigemasa Y, Matsuda Y, Sakazawa C, Matsuura T (1977) Formose reactions. ii. the photochemical formose reaction. *Bull Chem Soc Japan* 50(1):222–226

- Snytnikova OA, Simonov AN, Pestunov OP, Parmon VN, Tsentalovich YP (2006) Study of the photoinduced formose reaction by flash and stationary photolysis. *Mendeleev Commun* 16(1):9–11
- Srisanga S, ter Horst JH (2010) Racemic compound, conglomerate, or solid solution: phase diagram screening of chiral compounds. *Cryst Growth Des* 10(4):1808–1812
- Stovbun S, Skoblin A, Mikhailov A, Grishin M, Shub B, Zanin A, Shashkin D (2012) Experimental investigation of anisometric chiral phase xerogel. *Rus J Phys Chem B* 7(9–10):531–538
- Stovbun SV, Skoblin AA, Zlenko DV (2018) Self assembly and gelation in solutions of chiral *n*-trifluoroacetylated α -aminoalcohols. *Chem Phys* 508:34–44
- Sweeley C, Bentley R, Makita M, Wells W (1963) Gas-liquid chromatography of trimethylsilyl derivatives of sugars and related substances. *J Am Chem Soc* 85(16):2497–2507
- Tverdislov VA, Malyshko E, Il'chenko S, Zhulyabina O, Yakovenko L (2017) A periodic system of chiral structures in molecular biology. *Biophysics* 62(3):331–341
- Viedma C (2005) Chiral symmetry breaking during crystallization: complete chiral purity induced by nonlinear autocatalysis and recycling. *Chem Rev Lett* 94(6):065504
- Viedma C (2007) Chiral symmetry breaking and complete chiral purity by thermodynamic-kinetic feedback near equilibrium: implications for the origin of biochirality. *Astrobiol* 7(2):312–319
- Weast RC (1974) *CRC handbook of chemistry and physics: a ready-reference book of chemical and physical data*. CRC Press, Cleveland
- Zlenko DV, Zanin AM, Skoblin AA, Tverdislov VA, Stovbun SV (2019) Spontaneous resolution in racemic solutions of *N*-trifluoroacetylated α -aminoalcohols. *Mol Struct* 1183:8–13

Publisher's Note Springer Nature remains neutral with regard to jurisdictional claims in published maps and institutional affiliations.